ABSORBING BOUNDARY CONDITIONS WITH ZERO REFLECTION ANGLES FOR COMPRESSIONAL AND SHEAR INCIDENT WAVES

Jianwei Zhou and Nader Saffari
Department of Mechanical Engineering
University College London
Torrington Place
London WC1E 7JE
England

INTRODUCTION

The technique of artificial absorbing boundaries is often applied in the numerical modelling of wave propagation and other related numerical studies of ultrasonic NDE. For a physical problem with an unbounded spatial domain, the introduction of artificial boundaries to bound the computational domain can be vital for a successful numerical solution. Even for problems with bounded spatial domains, the introduction of artificial absorbing boundaries that localize the area of interest can reduce the computing cost and allow limited computer resources to achieve more. It is particularly so in ultrasonic NDE where the field near the scatterers or transducers is normally of interest.

Artificial absorbing boundaries are introduced through special boundary conditions that filter out waves propagating outwards from the area of interest. Thus the calculation of the wave field needs only to be performed on a computational domain much smaller than the physical domain. In recent years, there have been many contributions in the development of absorbing boundary conditions with a variety of techniques employed for achieving energy absorption, see [1,3,6-8]. The review article [2] provides more background on the subject.

The artificial boundaries that we are going to deal with in this work are $z = (z_0)_-$, $z = (z_0)_+$, $x = (x_0)_-$ and $x = (x_0)_+$. Here, $z = (z_0)_-$ is defined as the boundary $z = z_0$ that bounds the computational domain $z \leq z_0$. The other three boundaries can be described similarly. In the following sections, we shall mainly establish our analysis and develop absorbing boundary conditions for the artificial boundary $z = (z_0)_-$. Results for other types of artificial boundaries will be discussed also.

The elastic wave equations concerned in this study are in the form of

$$\underline{u}_{tt} = \begin{bmatrix} \alpha^2 & 0 \\ 0 & \beta^2 \end{bmatrix} \underline{u}_{xx} + \begin{bmatrix} 0 & \alpha^2-\beta^2 \\ \alpha^2-\beta^2 & 0 \end{bmatrix} \underline{u}_{xz} + \begin{bmatrix} \beta^2 & 0 \\ 0 & \alpha^2 \end{bmatrix} \underline{u}_{zz}, \qquad \underline{u} = \begin{bmatrix} U \\ W \end{bmatrix}. \tag{1}$$

The parameters α and β are the compressional and shear wave velocities, respectively. Solutions of the elastic wave equation (1) may be obtained by superpositioning a collection of compressional wave vectors

Review of Progress in Quantitative Nondestructive Evaluation, Vol. 15
Edited by D.O. Thompson and D.E. Chimenti, Plenum Press, New York, 1996

$$\underline{u} = \phi(\xi x + \eta z - \alpha t)\begin{bmatrix}\xi\\ \eta\end{bmatrix}, \tag{2}$$

and shear wave vectors

$$\underline{u} = \phi(\xi x + \eta z - \beta t)\begin{bmatrix}\eta\\ -\xi\end{bmatrix}, \tag{3}$$

where $\phi(s)$ in the above expressions is some suitable univariate potential function.

REFLECTION COEFFICIENTS AND ZERO REFLECTION ANGLES

The absorbing boundary conditions that we are looking for are in the form of homogeneous partial differential equations with constant matrix coefficients. Generally, they may be expressed as

$$L(\partial_t, \partial_x, \partial_z)\underline{u} = \underline{0} \tag{4}$$

where $L(p,q,r)$ is a homogeneous 2×2 matrix polynomial.

Let us consider the artificial boundary $z = (z_0)\_$ and assume $z_0 = 0$ without the loss of generality. When a compressional incident wave

$$\phi(\xi x + \eta z - \alpha t)\begin{bmatrix}\xi\\ \eta\end{bmatrix}, \quad \xi = \sin\theta, \quad \eta = \cos\theta, \quad -\frac{\pi}{2} < \theta < \frac{\pi}{2}, \tag{5}$$

that travels in the positive-z direction hits the boundary $z = (z_0)_-$, with θ being the angle of incidence, two reflected waves are generated for the boundary condition (4) to be satisfied. Thus the solution to both the elastic wave equation and the boundary condition will be

$$\underline{u} = \phi(\xi x + \eta z - \alpha t)\begin{bmatrix}\xi\\ \eta\end{bmatrix} + R_{pp}\,\phi(\xi x - \eta z - \alpha t)\begin{bmatrix}\xi\\ -\eta\end{bmatrix} + R_{ps}\,\phi(\xi x - \eta' z - \alpha t)\begin{bmatrix}-\eta'\\ -\xi\end{bmatrix}, \tag{6}$$

where $\eta'\eta > 0$ and $\alpha^2(\xi^2 + \eta^2) = \beta^2(\xi^2 + \eta'^2)$. We shall call R_{pp} the compressional reflection coefficient and R_{ps} the shear reflection coefficient for a compressional incident wave, respectively. Similarly for a shear incident wave, the solution will be

$$\underline{u} = \phi(\xi x + \eta z - \beta t)\begin{bmatrix}\eta\\ -\xi\end{bmatrix} + R_{ss}\,\phi(\xi x - \eta z - \beta t)\begin{bmatrix}-\eta\\ -\xi\end{bmatrix} + R_{sp}\,\phi(\xi x - \eta'' z - \beta t)\begin{bmatrix}\xi\\ -\eta''\end{bmatrix}, \tag{7}$$

where $Re(\eta''\eta) > 0$ and $\beta^2(\xi^2 + \eta^2) = \alpha^2(\xi^2 + \eta''^2)$. We call R_{ss} the shear reflection coefficient and R_{sp} the compressional reflection coefficient for a shear incident wave, respectively. Substituting (6) and (7) into (4), we obtain the following expressions for the reflection coefficients as functions of the angle of incidence θ

$$\begin{bmatrix}R_{pp}(\theta)\\ R_{ps}(\theta)\end{bmatrix} = -\left[L(-\alpha,\xi,-\eta)\begin{bmatrix}\xi\\ -\eta\end{bmatrix} \quad L(-\alpha,\xi,-\eta')\begin{bmatrix}-\eta'\\ -\xi\end{bmatrix}\right]^{-1} L(-\alpha,\xi,\eta)\begin{bmatrix}\xi\\ \eta\end{bmatrix} \tag{8}$$

and

$$\begin{bmatrix} R_{ss}(\theta) \\ R_{sp}(\theta) \end{bmatrix} = -\left[L(-\beta,\xi,-\eta)\begin{bmatrix} -\eta \\ -\xi \end{bmatrix} \quad L(-\beta,\xi,-\eta'')\begin{bmatrix} \xi \\ -\eta'' \end{bmatrix} \right]^{-1} L(-\beta,\xi,\eta)\begin{bmatrix} \eta \\ -\xi \end{bmatrix}. \tag{9}$$

An angle θ_p is a zero reflection angle for compressional incident waves if

$$R_{pp}(\theta_p) = 0\,, \qquad R_{ps}(\theta_p) = 0\,. \tag{10}$$

Similarly, if

$$R_{ss}(\theta_s) = 0\,, \qquad R_{sp}(\theta_s) = 0\,, \tag{11}$$

then θ_s is called a zero reflection angle for shear incident waves. From (8) and (9), we deduce that (10) and (11) are equivalent to

$$L(-\alpha, \sin\theta_p, \cos\theta_p)\begin{bmatrix} \sin\theta_p \\ \cos\theta_p \end{bmatrix} = \underline{0} \quad \text{and} \quad L(-\beta, \sin\theta_s, \cos\theta_s)\begin{bmatrix} \cos\theta_s \\ -\sin\theta_s \end{bmatrix} = \underline{0}\,. \tag{12}$$

PRACTICAL SECOND ORDER ABSORBING BOUNDARY CONDITIONS

We examine the propagation of the following wave

$$\underline{u} = \phi(\xi x + \eta z - \omega t)\,\underline{g} \tag{13}$$

where

$$\underline{g} = \begin{bmatrix} \xi \\ \eta \end{bmatrix} \text{ if } \omega^2 = \alpha^2(\xi^2+\eta^2)\,, \qquad \text{or}\,, \qquad \underline{g} = \begin{bmatrix} \eta \\ -\xi \end{bmatrix} \text{ if } \omega^2 = \beta^2(\xi^2+\eta^2)\,. \tag{14}$$

It can be seen that the sign of the term $\omega\eta$ determines the direction of propagation. The wave travels in the positive-z direction if $\omega\eta > 0$ and in the negative-z direction if $\omega\eta < 0$.

In order to remove the reflections from the artificial boundary $z = (z_0)_-$, we need absorbing boundary conditions that can differentiate waves travelling in these directions. Thus an absorbing boundary condition in the form of a second order partial differential equation should contain the term $\underline{u}_{tz}$. It is also desirable that absorbing boundary conditions are in simple differential equation forms that are comparable with the elastic wave equation (1). We therefore seek absorbing boundary conditions (4) with

$$L(p,q,r) = \begin{bmatrix} 1 & 0 \\ 0 & 1 \end{bmatrix} pr + \begin{bmatrix} a_1 & 0 \\ 0 & a_2 \end{bmatrix} q^2 + \begin{bmatrix} 0 & b_1 \\ b_2 & 0 \end{bmatrix} qr + \begin{bmatrix} c_1 & 0 \\ 0 & c_2 \end{bmatrix} r^2\,, \tag{15}$$

that is

$$L(\partial_t, \partial_x, \partial_z)\underline{u} := \underline{u}_{tz} + \begin{bmatrix} a_1 & 0 \\ 0 & a_2 \end{bmatrix} \underline{u}_{xx} + \begin{bmatrix} 0 & b_1 \\ b_2 & 0 \end{bmatrix} \underline{u}_{xz} + \begin{bmatrix} c_1 & 0 \\ 0 & c_2 \end{bmatrix} \underline{u}_{zz} = \underline{0}\,. \tag{16}$$

The unknown elements of coefficient matrices may be determined by requiring zero reflections for certain angles of incidence. For two arbitrarily prescribed angles θ_p and θ_s, we impose

$$R_{pp}(\theta) = 0\,, \quad R_{ps}(\theta) = 0\,, \quad \text{for} \quad \theta = -\theta_p\,, 0\,, \theta_p \tag{17}$$

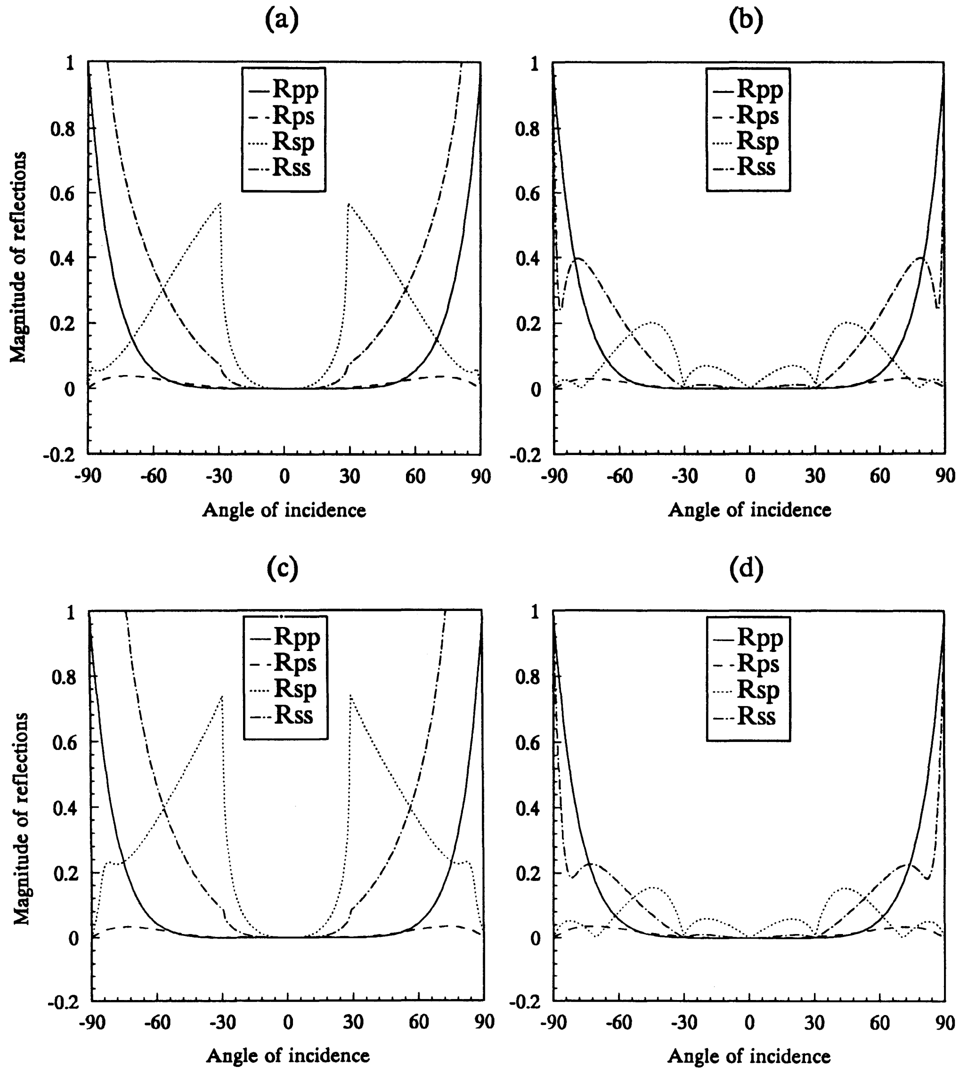

Figure 1. Magnitudes of the four reflection coefficients for (a) $\theta_p = 0°$ and $\theta_s = 0°$, (b) $\theta_p = 30°$ and $\theta_s = 30°$, (c) $\theta_p = 30°$ and $\theta_s = 0°$, and (d) $\theta_p = 0°$ and $\theta_s = 30°$.

and

$$R_{ss}(\theta) = 0\,, \quad R_{sp}(\theta) = 0\,, \quad \text{for} \quad \theta = -\theta_s\,, 0\,, \theta_s\,. \tag{18}$$

Then by solving three pairs of the vector equations of (12) with L defined by (15), we obtain

$$a_1 = \alpha\cos\theta_p - \beta\frac{\cos^2\theta_p}{1+\cos\theta_s}, \quad a_2 = \beta\cos\theta_s - \alpha\frac{\cos^2\theta_s}{1+\cos\theta_p},$$

$$b_1 = \alpha\cos\theta_p - \beta\frac{\cos^2\theta_p + \cos\theta_s}{1+\cos\theta_s}, \quad b_2 = -\beta\cos\theta_s + \alpha\frac{\cos\theta_p + \cos^2\theta_s}{1+\cos\theta_p}, \tag{19}$$

$$c_1 = \beta, \quad c_2 = \alpha.$$

Equation (16) with matrix elements given by (19) is our new absorbing boundary condition for the artificial boundary $z = (z_0)_-$. Plots of reflection coefficients versus angles of incidence for aluminium are displayed in Figure 1 for $(\theta_p, \theta_s) = (0°, 0°)$, $(30°, 30°)$, $(30°, 0°)$ and $(0°, 30°)$. The condition for $z = (z_0)_+$ can be derived formally by replacing α and β by $-\alpha$ and $-\beta$, respectively. For vertical artificial boundaries, absorbing boundary conditions are obtained by exchanging x with z and U with W.

We point out that the class of new absorbing boundary conditions presented here is the generalization of our earlier work [7] which corresponds to the case $\theta_s = \theta_p = \theta_1$. The main improvement lies in the fact that the angles of zero reflection can now be assigned to absorbing boundary conditions independently for compressional and shear incident waves. It therefore yields an additional degree of freedom for the reduction of unwanted reflected waves. This becomes particularly important after studying the plots of reflection coefficients in Figure 1. The magnitudes of reflection coefficients R_{pp} and R_{ps}, due to compressional incident waves, are small for a reasonably large range of angles of incidence. However, reflection coefficients R_{ss} and R_{sp}, due to shear incident waves, do not exhibit the same property. By adjusting the values of θ_s and θ_p, the magnitudes of reflection coefficients R_{ss} and R_{sp} may be minimized, as indicated in Figure 1.

A NUMERICAL EXAMPLE

To demonstrate the effect of our new absorbing boundary conditions, we consider the problem where a rectangular void appears in the middle of a solid formed by aluminium. The scattered wave field due to the presence of such a defect is to be calculated. The computational domain is chosen to be a larger rectangle that has sides parallel to the sides of the rectangular defect. Absorbing boundary conditions are imposed on all sides of the computational domain. The sides of the rectangular defect are constrained as stress-free surfaces. The calculation of the wave field will be carried out through a forward iteration in time.

Let $\underline{u}_{i,j,k} = \underline{u}(x_0 + i\Delta x, z_0 + j\Delta z, t_0 + k\Delta t)$ and denote the difference operators

$$(D_+^x)\underline{u}_{i,j,k} = \underline{u}_{i+1,j,k} - \underline{u}_{i,j,k}, \quad (D_-^x)\underline{u}_{i,j,k} = \underline{u}_{i,j,k} - \underline{u}_{i-1,j,k}, \quad (D_0^x)\underline{u}_{i,j,k} = \underline{u}_{i+1,j,k} - \underline{u}_{i-1,j,k},$$

$$(D_+^z)\underline{u}_{i,j,k} = \underline{u}_{i,j+1,k} - \underline{u}_{i,j,k}, \quad (D_-^z)\underline{u}_{i,j,k} = \underline{u}_{i,j,k} - \underline{u}_{i,j-1,k}, \quad (D_0^z)\underline{u}_{i,j,k} = \underline{u}_{i,j+1,k} - \underline{u}_{i,j-1,k},$$

$$(D_+^t)\underline{u}_{i,j,k} = \underline{u}_{i,j,k+1} - \underline{u}_{i,j,k}, \quad (D_-^t)\underline{u}_{i,j,k} = \underline{u}_{i,j,k} - \underline{u}_{i,j,k-1}, \quad (D_0^t)\underline{u}_{i,j,k} = \underline{u}_{i,j,k+1} - \underline{u}_{i,j,k-1}. \tag{20}$$

We now summarize the finite difference formulation for computing the wave field. At interior body nodes, the discretized wave equation is used which gives

$$\underline{u}_{i,j,k+1}=2\underline{u}_{i,j,k}-\underline{u}_{i,j,k-1}+\frac{\gamma_x\gamma_z}{4}\begin{bmatrix}0 & \alpha^2-\beta^2\\ \alpha^2-\beta^2 & 0\end{bmatrix}(D_0^x)(D_0^z)\underline{u}_{i,j,k}$$

$$+\gamma_x^2\begin{bmatrix}\alpha^2 & 0\\ 0 & \beta^2\end{bmatrix}(D_+^x)(D_-^x)\underline{u}_{i,j,k}+\gamma_z^2\begin{bmatrix}\beta^2 & 0\\ 0 & \alpha^2\end{bmatrix}(D_+^z)(D_-^z)\underline{u}_{i,j,k}, \tag{21}$$

where $\gamma_x=\Delta t/\Delta x$ and $\gamma_z=\Delta t/\Delta z$. New composed stress-free boundary conditions [4,5] with a slight modification are implemented for boundaries of the rectangular void in the middle. For example, the formula for the lower edge is

$$\underline{u}_{i,j,k+1}=2\underline{u}_{i,j,k}-\underline{u}_{i,j,k-1}+2\gamma_z^2\begin{bmatrix}\beta^2 & 0\\ 0 & \alpha^2\end{bmatrix}(D_+^z)\underline{u}_{i,j,k}+\gamma_x^2\begin{bmatrix}\alpha^2 & 0\\ 0 & \beta^2\end{bmatrix}(D_+^x)(D_-^x)\underline{u}_{i,j,k}$$

$$+\frac{\gamma_x\gamma_z}{2}\begin{bmatrix}0 & \alpha^2-\beta^2\\ \alpha^2-\beta^2 & 0\end{bmatrix}(D_0^x)(D_+^z)\underline{u}_{i,j,k}+\gamma_x\gamma_z\begin{bmatrix}0 & \beta^2\\ \alpha^2-2\beta^2 & 0\end{bmatrix}(D_0^x)\underline{u}_{i,j,k}. \tag{22}$$

Absorbing boundary condition (16) is first combined with elastic wave equation (1) to

$$\underline{u}_{tt}=-\begin{bmatrix}\beta & 0\\ 0 & \alpha\end{bmatrix}\underline{u}_{tz}+\begin{bmatrix}\alpha^2-\beta a_1 & 0\\ 0 & \beta^2-\alpha a_2\end{bmatrix}\underline{u}_{xx}+\begin{bmatrix}0 & \alpha^2-\beta^2-\beta b_1\\ \alpha^2-\beta^2-\alpha b_2 & 0\end{bmatrix}\underline{u}_{xz} \tag{23}$$

and then implemented as

$$\underline{u}_{i,j,k+1}=2\underline{u}_{i,j,k}-\underline{u}_{i,j,k-1}+\frac{\gamma_x\gamma_z}{2}\begin{bmatrix}0 & \alpha^2-\beta^2-\beta b_1\\ \alpha^2-\beta^2-\alpha b_2 & 0\end{bmatrix}(D_0^x)(D_-^z)\underline{u}_{i,j,k}$$

$$-\gamma_z\begin{bmatrix}\beta & 0\\ 0 & \alpha\end{bmatrix}(D_-^t)(D_-^z)\underline{u}_{i,j,k}+\gamma_x^2\begin{bmatrix}\alpha^2-\beta a_1 & 0\\ 0 & \beta^2-\alpha a_2\end{bmatrix}(D_+^x)(D_-^x)\underline{u}_{i,j,k} \tag{24}$$

for the lower artificial boundary. Absorbing boundary conditions for other artificial boundaries are implemented similarly. Corner nodes formed by the intersections of horizontal and vertical artificial boundaries are implemented as absorbing corners where the horizontal component of $\underline{u}$ is constrained by the vertical absorbing boundary condition and the vertical component by the horizontal condition. Corners of the rectangular voids are discretized as modified body nodes with $2(D_0^x)(D_0^z)\underline{u}_{i,j,k}$ replaced by $(D_-^x)(D_-^z)\underline{u}_{i,j,k}+(D_+^x)(D_+^z)\underline{u}_{i,j,k}$ or $(D_+^x)(D_-^z)\underline{u}_{i,j,k}+(D_-^x)(D_+^z)\underline{u}_{i,j,k}$ to avoid the use of points inside the void.

A vertical compressional pulse that travels upwards is introduced in the lower part of the computational domain. The pulse is regarded as an analytical solution when no defect is present and is available at any time level. The scattered wave due to the void is to be computed. Absorbing boundary conditions only apply to the scattered wave field. Figure 2 shows the wave field at $t=t_0$, $t=t_0+75\Delta t$ and $t=t_0+125\Delta t$. The parameters for absorbing boundary conditions used in the calculation are $\theta_p=0°$ and $\theta_s=30°$.

The l_2-norm of the wave field in the computational domain

$$S_k=\left(\sum_{i,j}\underline{u}_{i,j,k}\cdot\underline{u}_{i,j,k}\right)^{1/2} \tag{25}$$

measures the remaining energy in the domain and indicates the effectiveness of absorbing boundary conditions at the artificial boundaries that bound the computational domain.

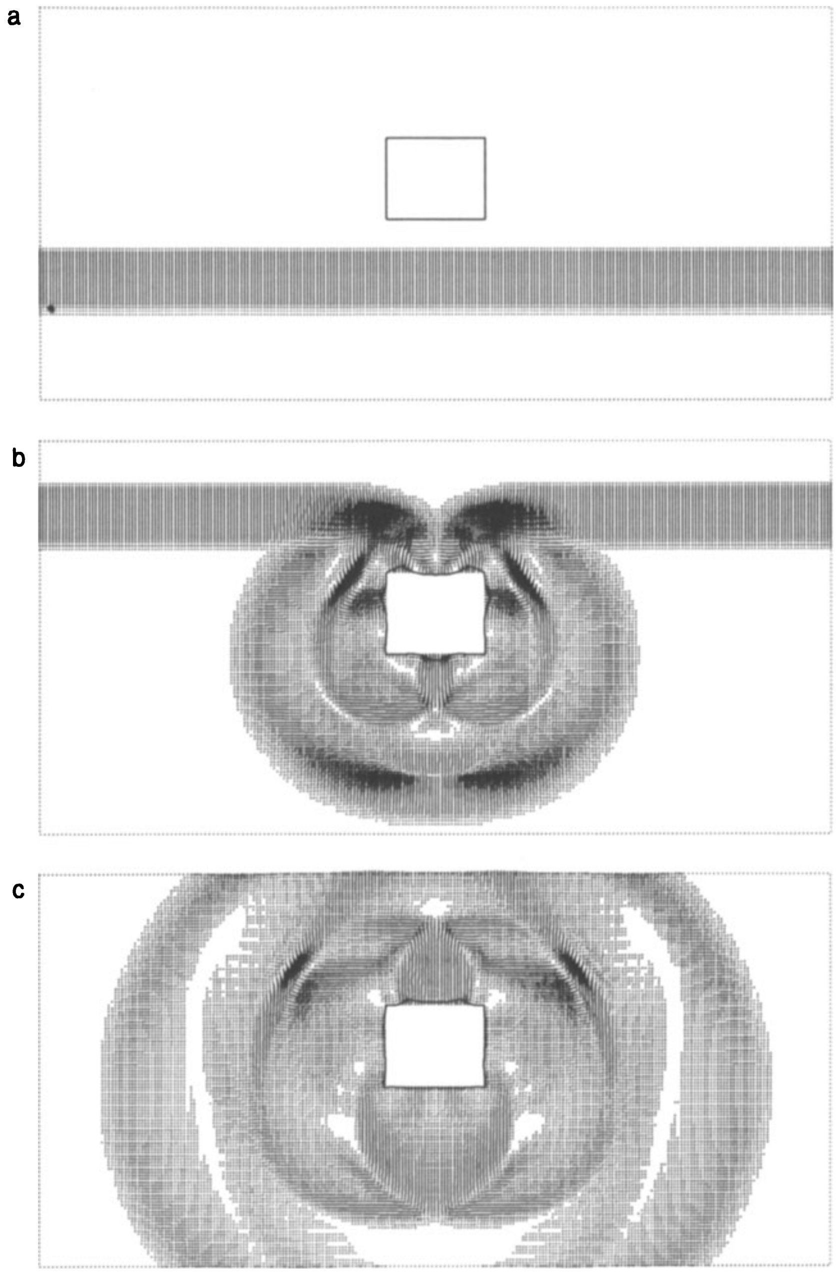

Figure 2. Wave field at (a) $t = t_0$, (b) $t = t_0 + 75\Delta t$ and (c) $t = t_0 + 125\Delta t$.

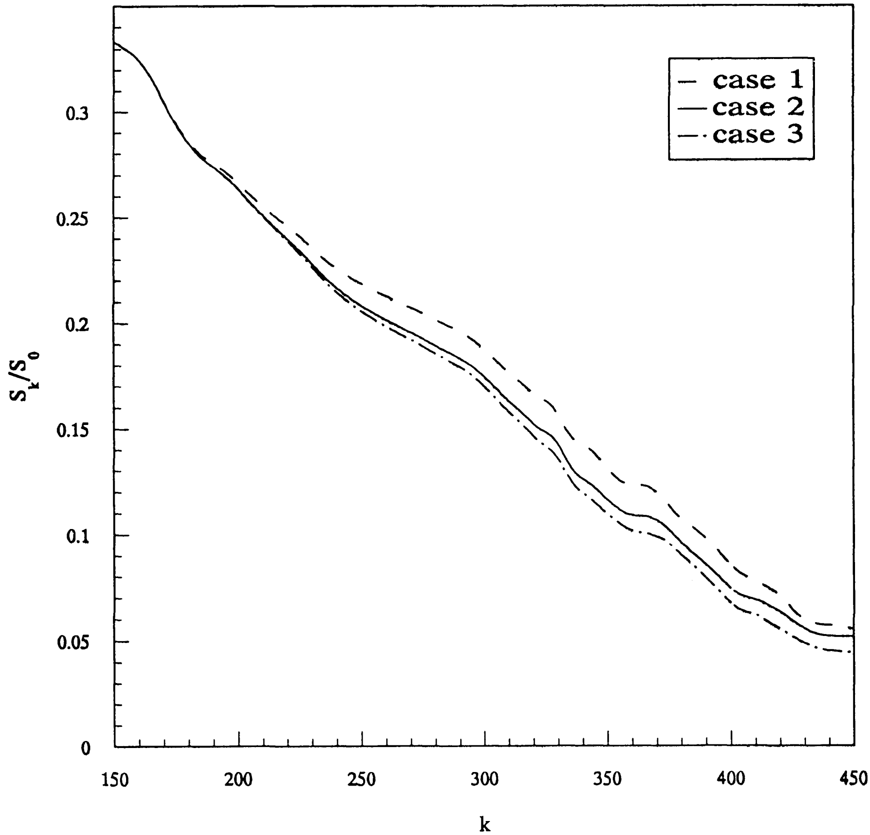

Figure 3. Remaining energy in three cases of absorbing boundary conditions.

The display in Figure 3 covers three cases to illustrate a simple comparison of our new conditions with two existing ones. Case 1 is Stacey's P4 condition [8] where $\theta_p = \theta_s = 0°$. Case 2 is the condition from our earlier work [7] with $\theta_p = \theta_s = 30°$. An improvement over Stacey's condition is shown. Case 3 is the new condition developed in this study with $\theta_p = 0°$ and $\theta_s = 30°$. A further improvement is observed.

ACKNOWLEDGEMENTS

This work was performed with the support of a grant awarded by the Engineering and Physical Sciences Research Council, UK.

REFERENCES

1. R. Clayton and B. Engquist, Bull. Seismol. Soc. Am. 67, 1529 (1977).
2. D. Givoli, J. Comput. Phys. 94, 1 (1991).
3. R. L. Higdon, J. Comput. Phys. 101, 386 (1992).
4. A. Ilan, J. Comput. Phys. 29, 389 (1978).
5. A. Ilan and D. Loewenthal, Geophys. Prosp. 24, 431 (1976).
6. R. G. Keys, Geophysics 50, 892 (1985).
7. N. Saffari and J. Zhou, in *Review of Progress in QNDE,* Vol. 14, eds. D. O. Thompson and D. E. Chimenti (Plenum, New York, 1995), p. 211.
8. R. Stacey, Bull. Seismol. Soc. Am. 78, 2089 (1988).